

Using Direct Water Saturation for Sensitive Detection of Iron in the Human Brain

S. A. Smith^{1,2}, J. W. Bulte^{2,3}, and P. C. van Zijl^{1,2}

¹F.M. Kirby Research Center, Kennedy Krieger Institute, Baltimore, MD, United States, ²Department of Radiology, Johns Hopkins University, Baltimore, MD, United States, ³Institute for Cell Engineering, Johns Hopkins University, Baltimore, MD, United States

Introduction: Iron is one of the most important and abundant physiological metals, occurring endogenously in almost all organisms. Most brain iron is non-heme and is stored primarily in the form of ferritin. Physiologically, different gray matter structures of the brain are known to have varying iron content (1). Increased presence of non-heme iron in the brain is also known to be linked to a variety of devastating neurodegenerative disorders such as Alzheimer's (AD) and Parkinson's disease (PD) (2). Additionally, iron oxide-labeling is also a popular approach for cell tracking (3). Current iron studies are based on T2/T2* MRI. Recently, when performing MTR imaging at 3T, we noticed sensitivity of the contrast to iron concentration in gray matter regions (4). At the same time, an off-resonance irradiation approach was presented that yielded signal attenuation which was related to iron concentration in SPIO-doped phantoms (5). The mechanism is that the water line broadens due to the iron-induced shortening of T2/T2* with the frequency-dependent RF irradiation giving rise to varying degrees of direct water saturation. Using ferritin-doped agarose phantoms, we show that direct saturation can be used to determine iron content. We further study this *in vivo* and examine deep grey matter structures for their correlation with the age-adjusted non-heme iron concentration taken from the literature (1).

Methods: Simulation: Simulation of the Bloch Equations describing the transverse and longitudinal magnetization modified for a direct water saturation experiment was performed to optimize acquisition methods prior to examination. Since T2* decreases with increasing iron concentration, the sequence parameters (RF amplitude, B₁, duration of pulse, t_{sat}, and TR) were optimized to yield the largest difference in the direct saturation effect for fractional change in T2*. **Experimental: In Vitro:** Horse spleen ferritin (14.24 mg Fe/ml) was added to 2% agarose to yield 14 iron concentrations with a range 0-45mg/100g agarose. MRI experiments were performed on a 3T Intera system (Philips Medical Systems, Best, The Netherlands) with body coil transmission and SENSE head coil reception. Direct water saturation images were obtained at ω = 110 Hz, S(ω), using a 3D-spoiled gradient echo, TR/TE/α = 600ms/2.1ms/90°, with a 250 ms non-selective block saturation pulse (B₁ = 0.6μT) and multi-shot echo planar imaging. The percent direct effect was calculated similarly to MTR, namely Direct Saturation Ratio: DSR = (1 - S_{sat}(ω)/S₀) where S₀ is the signal intensity in the absence of RF saturation. **In Vivo:** 3 healthy adults (22-30 yr) were scanned after written informed consent. In addition to the sequence performed above, other parameters were: FOV = 230x230x60 mm (ap,rl,fb), acquired resolution: 2x2x3 mm, total scan time 4min. The DSR was calculated. Examination of the regional DSR was performed by manually selecting 8 ROIs: parietal cortex (Crtx), caudate nucleus (CN), dentate nucleus

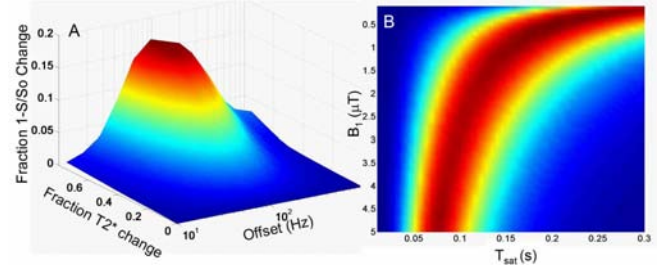


Fig 1: A) DSR as a function of fractional change in T₂ at t_{sat} = 300 ms, B₁ = 1.0μT. B) Location of maximal direct effect change (dark red) as function of B₁ and t_{sat} for offset = 110 Hz.

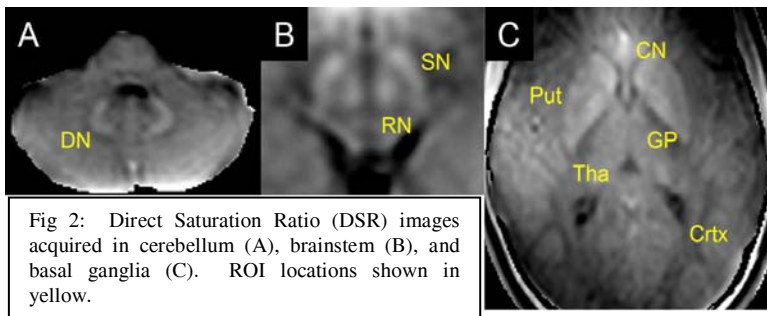


Fig 2: Direct Saturation Ratio (DSR) images acquired in cerebellum (A), brainstem (B), and basal ganglia (C). ROI locations shown in yellow.

and offset of the RF saturation pulse were chosen to be 0.6 μT, 250ms, and 110 Hz, respectively, for all subsequent experiments. It is important to note that these parameters are sufficient to avoid most MT effects and leave only direct water saturation contrast. *In vivo* DSR images (Fig 2 A-C) show very high contrast between grey matter regions in the cerebellum (Fig 2A), brainstem (Fig 2B), and basal ganglia (Fig 2C). ROI analysis shows a striking correlation between mean (3 volunteers) DSR and mean age-adjusted non-heme iron concentration (Fig 3 bottom, red line, R = 0.93; p < 0.001). Fig 3 top shows results of similar measurements performed in the ferritin-doped agarose phantoms with an excellent correlation of R = 0.99 and p < 0.001 (dotted lines indicate [Fe] range for healthy volunteers). This indicates that an off-resonance preparation can be used to elicit contrast based purely on water line broadening. A potential advantage of this approach is that since the iron-induced contrast is generated by a low power RF irradiation, it can be combined with any conventional imaging experiment to elicit a greater, specific contrast. Therefore, direct water saturation imaging could find utility in any part of the human body and in regions where low SNR complicates conventional T2* imaging. Note that while excellent correlations were found between direct water saturation and known, non-heme iron concentration *in vivo*, this technique is not specific for iron. In fact any shortening of T2/T2* will yield a similar effect. Nevertheless, due to the greater concentration of iron as compared to other substances that could cause similar effects, the hypothesis is that this technique can be used to detect changes in iron concentration due to chronic disease, or evaluate therapeutic intervention.

Conclusion: *In vivo* direct water saturation imaging of the brain at 3T revealed a strong correlation with the reported iron content. Similar examination in phantoms with known iron concentration confirmed this correlation. Direct effect imaging potentially could be applied to the study of diseases that show a pathologic increase in intracerebral iron concentration, such as Alzheimer's, Parkinson's and many others. A further potential application is detection and tracking of iron oxide-labeled cells.

References: 1) Hallgren B and Sourander P. J. Neurochemistry 1958. Vol 3: 41-51. 2) Schenk J and Zimmerman E. NMR Biomed. 2004;17:433-445. 3) Bulte JWM and Kraitchman DL. NMR Biomed 2004;17:484-499. 4) Smith SA, et al. MRM 2006; 56: 866-875. 5) Zurkiya O, et al. MRM 2006; 56: 726-732.

Grant Acknowledgement: NIH/NIBIB (5R21EB000991), NIH/NCRR (RR015241).

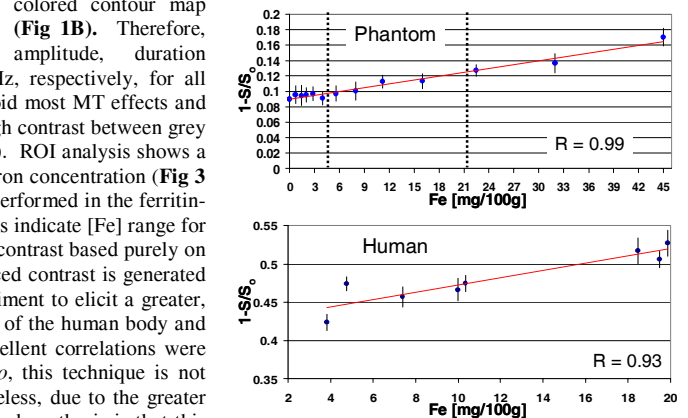


Fig. 3: (Top) mean DSR vs. known [Fe] in ferritin-doped phantoms. Dotted line indicates range of normal *in vivo* [Fe]. (Bottom) Regional mean DSR vs. age adjusted non-heme iron (from ref 1). Mean values averaged over 3 volunteers.